Dislocation strain field in ultrathin bonded silicon wafers studied by grazing incidence x-ray diffraction

J. Eymery
CEA/Grenoble, Département de Recherche Fondamentale sur la Matière Condensée/SP2M/SiNaPS, 17 rue des Martyrs, 38054 Grenoble Cedex 9, France

D. Buttard
CEA/Grenoble, Département de Recherche Fondamentale sur la Matière Condensée/SP2M/SiNaPS, 17 rue des Martyrs, 38054 Grenoble Cedex 9, France and Université Joseph Fourier, France

F. Fournel and H. Moriceau
CEA/Grenoble, LETI, Département des Technologies Silicium, 17 rue des Martyrs, 38054 Grenoble Cedex 9, France

G. T. Baumbach
Fraunhofer Institut für Zerstörungsfrei Prüfverfahren, EADQ, Krügerstrasse, 22, D-01326 Dresden, Germany

D. Lübbert*
ESRF, Grenoble Cedex, France

(Received 11 October 2001; revised manuscript received 31 January 2002; published 12 April 2002)

An ultrathin silicon layer (16 nm) bonded onto a silicon wafer is studied by grazing incidence x-ray diffraction. We measure satellite peaks around the {220} reflections coming from two periodic dislocation networks localized at the bonding interface. These lateral superlattice peaks are explained with a simple continuum model, and their positions give information about the tilt and twist misalignment of the two crystals, as well as the nature and interactions between the dislocation arrays. The square symmetry of dissociated screw dislocations (twist) and the average alignment of the mixed dislocations (tilt) are observed. The analysis of the satellite truncation rods shows that the strain field is strong enough to affect the surface, and that the dissociation of screw dislocations has to be taken into account.

DOI: 10.1103/PhysRevB.65.165337 PACS number(s): 61.10.Eq, 61.72.Dd, 61.72.Mm, 81.05.Cy

I. INTRODUCTION

The achievement of substrates having regular nanometric patterning has attracted a lot of interest in recent years because of their potential use as template for the self-organized growth of semiconductor quantum dots. To pursue the race to miniaturization of electronic circuits, the challenge is now to control the size and the position of the dots. An original assembling technique using direct wafer bonding of a 100 mm (001) silicon wafer and a silicon on insulator (SOI) wafer has been used recently to obtain high quality ultrathin Si crystalline layers (~10 nm) onto Si substrates.[1,2] For a bonded interface between parallel (001) surfaces (i.e., no miscut), the twist ψ of the two surfaces induces a regular square grid of pure or dissociated screw dislocations, called hereafter twist interfacial dislocations (TWID's). Whereas a tilt angle θ (miscut angle of the bonded samples) induces 60° or mixed dislocations called tilt interfacial dislocations (TID's).[2,9] Both dislocations have Burgers vectors of the $a/2$ $\langle 110\rangle$ type ($|\mathbf{b}|=a/\sqrt{2}$) and are localized at the bonded interface with no emergence to the surface. It has been shown from continuum elasticity calculations[3,4] that the periodic dislocation strain field close to the surface may be used to obtain controlled surface patterning and to grow self-organized quantum dots with a narrow size distribution.[6] The propagation of the strain field to the surface has been confirmed experimentally by scanning tunneling microscopy with both the observation of a nanoscale surface patterning and the long-range ordering of Si quantum dots.[5,6] To understand this effect, these new substrates have been studied by several techniques. Transmission electron microscopy (TEM)[8,9] has been used to determine the nature of the dislocations and their interactions, x-ray specular reflectivity (XRSR) to study the surface roughness, the thickness fluctuations of the bonded layer along the full wafer, and the interface quality in terms of electronic density.[10] A quantitative analysis has proved that the interfacial layer resulting from the bonding was very thin and that its atomic density is significantly different from bulk Si only for large bonding twist angles (>5°). This decrease of density is mainly due to the presence of oxide precipitates for large twist (>5°) checked by high resolution TEM.[8,9] For smaller twist angles (<5°), the contrast is much lower, indicating the lack of extended defects (in particular no precipitate). Grazing incidence small angle diffuse scattering performed with synchrotron radiation[11] has shown that this technique was sensitive to the change of electronic density induced by the mixed dislocation or their decoration. Grazing incidence x-ray diffraction (GIXRD) gives complementary results in terms of quantitative measurements of the long-range order of the lateral displacement field and attenuation of the surface dislocation strain field as a function of the bonded layer thickness.

 ©2002 The American Physical Society

Previous measurements have been dedicated to thick twist-bonded samples[12,13] to study the periodic elastic modulation in two 350 μm thick crystals. In this two infinite media geometry, the amplitude of the modulation of atomic position decays exponentially with distance from the interface, and the characteristic thickness has been found to be inversely proportional to the twist angle. Within a free surface, the strain field of the buried dislocation network is only significant at the surface for a bonded layer thickness smaller than about half the dislocation array period,[3,4] and until now, no surface specific study involving so thin bonded films has been developed. In this article, the near surface strain field induced by ultrathin twist-bonded boundary obtained on a full 4-in. wafer will be quantitatively analyzed to understand the twist and tilt angle influence on the dislocation strain fields. The elaboration of the sample and the x-ray experimental setup will be first described before the analysis of the GIXRD measurements taking into account the goniometer resolution function. The diffraction features of the in-plane reflections will be explained with a continuum theory model, and the attenuation of the dislocation rods will be analyzed to have insight on the extension of the dislocation strain fields.

II. EXPERIMENTAL DETAILS

A HF-last process is used to bond at high temperature (>1100 °C) a standard 100 mm (001) silicon-on-insulator (SOI) on a (001) Si wafer.[2,9] Then, using the SOI buried oxide layer as a convenient etch stop layer, the SOI backside is removed and the SOI silicon layer is thinned. The advantage of this method is that the thinning of the Si bonded layer is started on a thin material with a known thickness. Using the combination of thermal oxidation and chemical etching, we obtain a very good thickness homogeneity of the final film[2] much better than what is achieved directly with thick single crystal thinning.[14] Typical thickness is about 10 nm, and the homogeneity is nearly given by the initial SOI thickness variation. Before the x-ray measurements, the samples are observed by plane-view and cross-section high resolution TEM to check the lack of extended defects and by classical two beam and weak beam conditions to visualize the interface dislocations and their regularity.[8,9] The upper ultrathin layer has an excellent crystalline quality and the dislocation networks are closely confined to the bonding interface. As stated previously, two network sets are observed. The first one consists of two orthogonal arrays of TWID's that are *dissociated* at low ψ in two 30° partials separated by an intrinsic stacking fault located on a {111} plane ($1/2[110] \rightarrow 1/6[211] + 1/6[12\bar{1}]$). The second set is a single array of TID's lines formed by mixed dislocation segments. The average lines are straight contrary to the meandering observed at low temperature bonding,[8] and the average orientation is related to the macroscopic miscuts of the initial wafers. One important feature is that *the screw array of* TWID's *is shifted by the half of its period* due to the interaction with mixed dislocations.[2,8] A detailed discussion about this dislocation interaction is given in Ref. 7. It is described in a convenient way by the Thomson tetrahedron joining the four {111} planes. The edges of this tetrahedron are formed by the Burgers vectors of the type $\frac{1}{2}\langle 110\rangle$ and the connections from the corners to the face centers of the triangles correspond to partial dislocation of the type $\frac{1}{6}\langle 112\rangle$. A schematic of screw and mixed (60° for simplicity) dislocation interactions is given in Fig. 1. In the example noted $CD \rightarrow CB + AC$ in Fig. 1, the screw and edge components induced by the twist (Burgers vector $\frac{1}{2}[110]$) and the tilt can react as $\frac{1}{2}[110] + [00\bar{1}] \rightarrow \frac{1}{2}[01\bar{1}] + \frac{1}{2}[10\bar{1}]$ where $\frac{1}{2}[01\bar{1}]$ and $\frac{1}{2}[10\bar{1}]$ correspond to Burgers vectors of 60° dislocations and $[00\bar{1}]$ accommodate the tilt. It is shown that the twist dislocation lines (full lines) are shifted by half of the period. Configuration (a) corresponds to an average direction of the mixed dislocations along the [010] direction and configuration (b) shows how an arbitrary direction of the average mixed dislocation line can be obtained. Note that we observe neither oxide precipitates nor threading dislocation in the sample we have analyzed by x ray, so that only the dislocation strain field perturbs the upper crystal. From ellipsometry measurement,[2] the thickness of the upper crystal is about 145±15 Å with homogeneity smaller than 5 Å on the x-ray footprint. The twist angle ψ is measured accurately by TEM (Ref. 9) with small fluctuations ($\psi = 1.33 \pm 0.15°$) because TWID's are geometrically necessary, the dissociation length of TWID's being about 33±3 Å. The measurement of the tilt

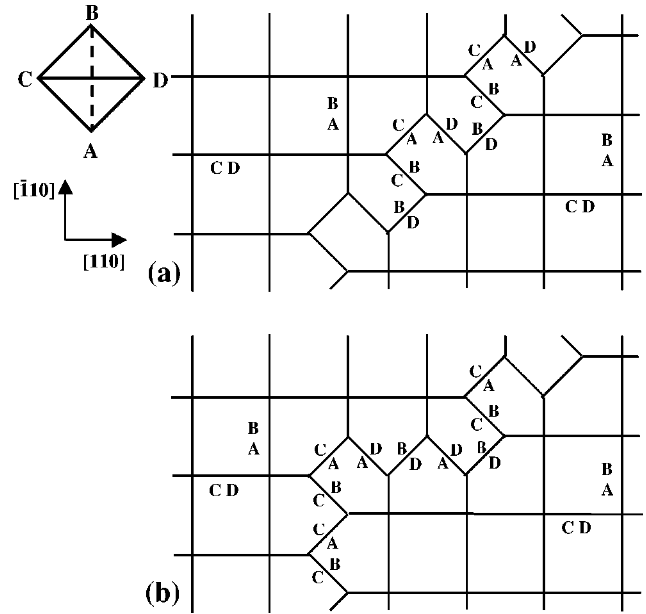

FIG. 1. Schematic of the interactions of a square network of screw dislocation with 60° dislocations having a component in the [001] direction to achieve a low energy configuration (the angle at the node is not fulfilled to have the lowest energy). The Burgers vectors are denoted by Thompson tetrahedron notation (see the inset at the left): $AB = \frac{1}{2}[\bar{1}10]$ and $CD = \frac{1}{2}[110]$ accommodate the twist, $CB = \frac{1}{2}[01\bar{1}]$, $CA = \frac{1}{2}[\bar{1}01]$, $AD = \frac{1}{2}[011]$, and $BD = \frac{1}{2}[101]$ have a component in the [001] direction and accommodate the tilt. Dislocation line directions are drawn with black lines (for the screw the line is along *CD* or *BA*). Configuration (a) corresponds to the [010] direction of the average mixed dislocation line, configuration (b) shows how it is possible to have a direction of the average mixed dislocation line different from [010] and [110].

angle is much sparse (only the global miscut of the wafers defines the tilt) and microscopy gives a very local information. For the same sample two image analysis give[2,9] $\theta \approx 0.43°$ and $\theta \approx 0.61°$.

GIXRD experiments have been performed at the ESRF ID 10A (Troïka) beamline at a wavelength $\lambda = 0.9322$ Å, the incident beam was well collimated to give a small divergence angle ($<0.006°$). A classic NaI scintillation detector was used to measure the diffraction pattern, and a position sensitive detector (PSD) to measure the dislocation truncation rods. The position and full width at half maximum of the diffraction peaks is the convolution between the node shape and the diffractometer resolution function, primarily controlled by the detector acceptance (130 μm$\times$1.5 mm with the NaI detector). The obliquely shaped resolution function is always tangent to the Ewald sphere and makes an angle θ_B (Bragg angle) with the momentum transfer vector q.

III. RESULTS AND DISCUSSION

With ω scan (see Fig. 2), we change only the in-plane angle ω between the incident beam and the diffraction planes perpendicular to the surface for a fixed Bragg position of the detector. The resolution function crosses the substrate (S) and layer (L) peaks along the x direction perpendicular to the momentum transfer vector, i.e., nearly along the S-L line corresponding to a $\langle 220 \rangle$ direction. It means that we have only a small peak broadening, and the twist angle measurement is not affected by the resolution function. For the TID's, the dislocation lines (and the average strain) are not aligned along the $\langle 220 \rangle$ direction because they have to respect the miscuts of the initial surfaces, so that we only measure the projections of the real peak positions.

Figure 2 shows two transversal q_x scans along the (220) and $(2-20)$ reflections for grazing incidence and emergence angles. As shown in Fig. 3, the diffraction profiles are composed of two sets of peaks, the first one is coming from the $(S)+(L)$ Bragg peaks and their satellites (circles), the second one corresponds to satellites centered on each peak of the first set (stars). These peaks *solely* result from the periodic strain field coming from the dislocation networks. Note that the TWID strain field corresponding to the two square networks cannot be measured along the same reflection (220) or $(2-20)$ because of the two perpendicular Burgers vectors. The general features can be explained in the framework of density perturbation of a continuous medium.[15] The dependence of the scattered amplitude is expanded as the function of the unperturbed density as

$$F(\mathbf{k}) = F_0(\mathbf{k}) + \frac{1}{(2\pi)^3} F_0(\mathbf{k}) \otimes A(\mathbf{k}),$$

where

$$\rho(\mathbf{r}) = \rho_0(\mathbf{r})[1 + a(\mathbf{r})],$$

$$F(\mathbf{k}) = \int \rho(\mathbf{r}) \exp(-i\mathbf{k}\cdot\mathbf{r}) d\mathbf{r},$$

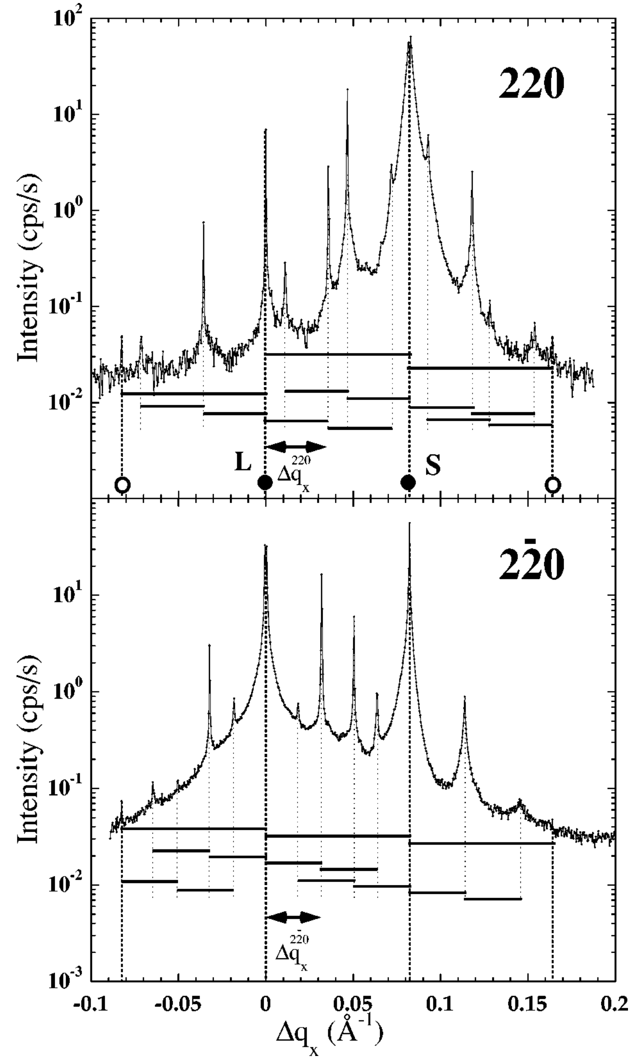

FIG. 2. Transversal ω-scan around the (2 2 0) and $(2\bar{2}0)$ reflections of an ultrathin bonded sample (twist $1.437 \pm 0.004°$, tilt 0.573 $\pm 0.005°$). $\Delta q_x \approx 4\pi/\lambda \Delta\omega \sin(\theta_B)$ where $\Delta\omega = \omega - \omega_0$, ω_0 is the substrate in-plane Bragg angle. S and L correspond to the peaks of the substrate and the thin layer. Incidence angle and emergence angles are respectively $\alpha_i = 0.17°$ (0.13°), $\alpha_f = 0.34°$ (0.26°). The lower part of each curve stresses the regularity of the networks and allows the indexation given in Fig. 3.

$$F_0(\mathbf{k}) = \int \rho_0(\mathbf{r}) \exp(-i\mathbf{k}\cdot\mathbf{r}) d\mathbf{r},$$

$$A(\mathbf{k}) = \int a(\mathbf{r}) \exp(-i\mathbf{k}\cdot\mathbf{r}) d\mathbf{r}.$$

With a harmonic plane wave $a(\mathbf{r}) = a_0 \cos[\mathbf{q}\cdot\mathbf{r} - \varphi_a]$, the lattice structure peaks $\mathbf{k}_i$ of $F_0(\mathbf{k})$ will produce extra peaks at $\mathbf{k}_i \pm \mathbf{q}$. The same formalism is applied to the combination of two perturbations $a(\mathbf{r})$ and $b(\mathbf{r})$ (also harmonic: $b(\mathbf{r}) = b_0 \cos[\mathbf{p}\cdot\mathbf{r} - \varphi_b]$) corresponding for example to the twist and tilt of the two crystals

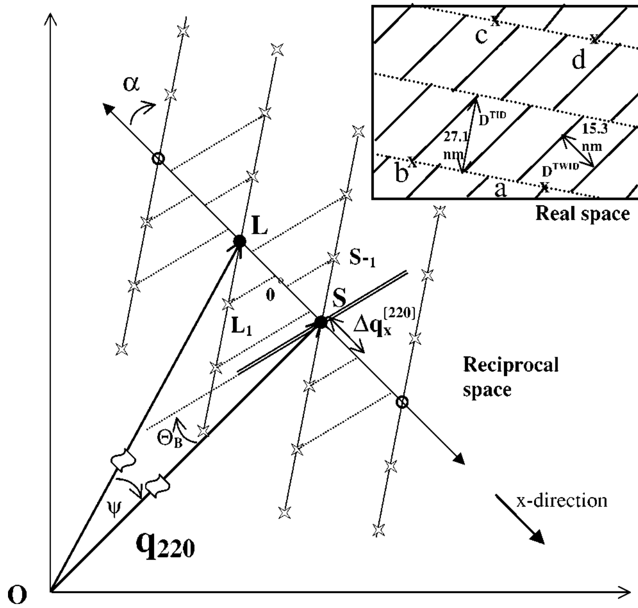

FIG. 3. Sketch of the lateral superlattice peaks around the (220) reflection (see Fig. 2). Open circles (stars) correspond to the measured twist (tilt) dislocation displacement peaks. For the sake of clarity, the full square network of screw dislocation is not drawn, but only the measured peaks. Due to the line and Burgers vectors of screw dislocation, the strain field of the TWID dislocation with the perpendicular orientation cannot be observed in the measurement (220) but only in the one around $(2-20)$ (see Fig. 2). Full circles noted L (S) correspond to the layer and substrate Bragg peaks. The letter O corresponds to the extinct 0-order peak of the twist dislocation network. Projection due to the resolution function (double lines centered on S) is shown with dotted lines. The inset shows a sketch of the real space to show the distances deduced from the x-ray analysis. The thick lines correspond to the dislocation lines of only one set of the TWID network (the dotted lines $a/2$ [220] Burgers vector) and the dotted lines to the average line of the mixed dislocations (TID) described in Fig. 1. Note the $D^{\mathrm{TWID}}/2$ shift induced by the interaction between TWID and TID.

$$F(\mathbf{k})=F_0(\mathbf{k})+\frac{1}{(2\pi)^3}F_0(\mathbf{k})\otimes[A(\mathbf{k})+B(\mathbf{k})]+\frac{1}{(2\pi)^6}F_0(\mathbf{k})\otimes A(\mathbf{k})\otimes B(\mathbf{k}).$$

The third term shows that extra peak of the first modulation $(\mathbf{k}_i\pm\mathbf{q})$ will also have satellites at $\mathbf{k}_i\pm\mathbf{q}\pm\mathbf{p}$. An estimation of the TWID satellite intensities can be reached with harmonic wave displacement[15] or with the twist boundary displacement field created by an array of nondissociated screw dislocations in a bicrystal.[16] The full quantitative analysis taking into account the surface and the real nature of dislocations (dissociated screw and mixed) can be performed with the calculated displacement fields deduced from the analytical model of Bonnet and Verger-Gaugry,[16,17] but these calculations are out of the scope of this paper.

The indexation of the diffraction peaks is shown in Figs. 2 and 3. As previously state, the momentum transfer $\Delta q_x\approx 0.0821$ Å^{-1} between (S) and (L) is equal for the two (220) and $(2-20)$ reflections and corresponds to $\Delta\omega\approx 1.437\pm 0.004°$ ($\Delta q_x\approx 2q_{110}\Delta\omega$). The period of the displacement field is given by[18] $D^{\mathrm{TWID}}=2\pi/(1/2\Delta q_x)=153\pm 0.3$ Å in full agreement with TEM measurements (168±18 Å). Note that the intensities of 0- and even-order peaks of the square TWID network are not measured in this sample, when they are clearly measured with samples having only a twist component. Twisted samples with $\psi\approx 0.44°, 1.0°$ ($\theta\approx 0°$), and $\psi\approx 180.44°$ ($\theta\approx 0.1°$) will be discussed in a forthcoming paper. This effect may be directly attributed to the dislocation interactions. As shown in the inset of Fig. 3, the TWID lines are shifted by $D^{\mathrm{TWID}}/2$ by the regular TID line network so that the displacement field period along the x direction is divided by two (i.e., doubled in the reciprocal space).

For the TID's we measure respectively $\Delta q_x^{[220]}=0.0356\pm 5.10^{-5}$ Å^{-1} (for $\omega=0°$ and $\omega=180°$) and $\Delta q_x^{[2-20]}=0.0318\pm 5.10^{-5}$ Å^{-1} (for $\omega=90°$ and $\omega=270°$). Simple geometrical calculations (see Fig. 3) show that $\Delta q_{\mathrm{real}}^{\mathrm{TID}}=\Delta q_x^{[220]}/(\cos\alpha+\sin\alpha\tan\theta_B)=\Delta q_x^{[2-20]}/(\sin\alpha-\cos\alpha\tan\theta_B)$, where $\theta_B=14.0512°$ is the (220) Bragg angle and α is the angle between the (S-L) line and the normal of the TID's lines. The direction of the TID is given by the relation $\cot g(\alpha-\theta_B)=\Delta q_x^{[220]}/\Delta q_x^{[2-20]}=1.1195$, so that $\alpha=55.82°$. It gives $\Delta q_{\mathrm{real}}^{\mathrm{TID}}=0.0463$ Å^{-1} and the distance between the TID's measured from GIXRD is $D^{\mathrm{TID}}=2\pi/(1/2\Delta q_{\mathrm{real}}^{\mathrm{TID}})=271.4\pm 0.5$ Å in agreement with the TEM value ($D^{\mathrm{TID}}=255\pm 42$ Å) that can be deduced from Fig. 1(b) of Ref. 2. The factor $\frac{1}{2}$ in the expression of D^{TID} is coming from the fact that only the even-order peaks of the TID network are measured (the center is taken at TWID satellite peaks). This effect, as well as the "extinction" of the even-order of the TWID network is also due to the interaction between TWID and TID networks. Note that another way to analyze the diffraction pattern induced by the two dislocation networks is to consider the O-centered reciprocal lattice defined in Fig. 3 by L, S_{-1}, S, L_1 (or a, b, c, d in the inset). Moreover in this sample, about one cell of the TWID square network is in between two TID lines, so that this sample corresponds to the case of an equal influence of the twist ($\psi=1.437°$) and of the tilt $(\theta=\arctan[a_{\mathrm{Si}}/(2D^{\mathrm{TID}})]=0.573°)$ angles.

The in-plane satellite diffraction peaks measured in the previous section are elongated in the direction perpendicular to the bonding plane. This is due to the truncation of the two crystals along the interface by the periodic displacement field. These truncation rods (TR's) can be measured accurately with a position sensitive detector (PSD) placed at the in-plane Bragg reflection angle by rotating the sample around its surface normal (ω scan). The (q_x,q_z) reciprocal space mapping (q_z normal to the surface) around the $(2\bar{2}0)$ reflections is shown in Fig. 4. It is clearly shown that the $(2+\delta,-2+\delta,l)$ truncation rods can be measured. Most TR's are coming from the TID (stars on Fig. 4), whereas only two weak TR's are coming from TWID peaks (circles on Fig. 4) showing that the strain induced by the screw dislocations are smaller than the mixed one. TR's intensities are fitted semiempirically[12] as a function of q_z with a squared Lorentzian function $I_i(q_z)=I_{i,0}[a_i/(a_i{}^2+q_z^2)]^2$. The choice

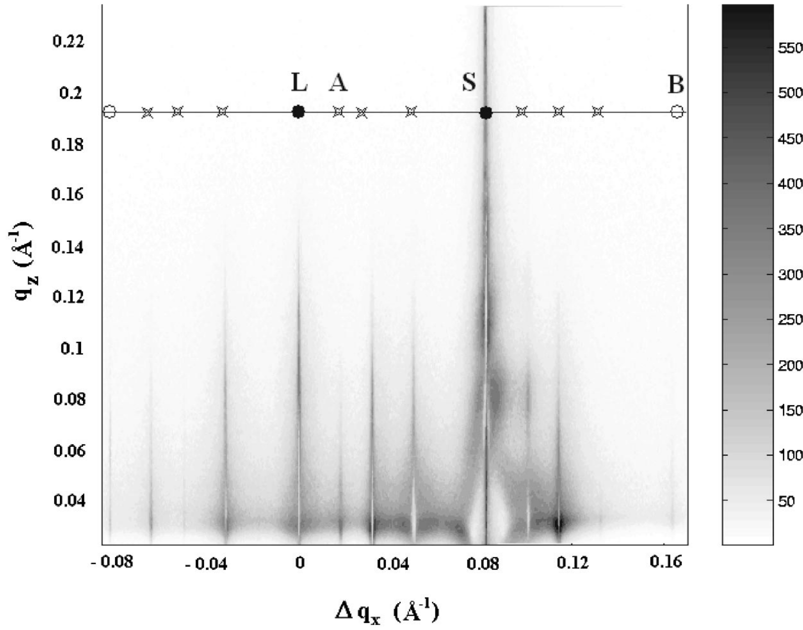

FIG. 4. Reciprocal space mapping around the $(2\bar{2}0)$ reflection of Fig. 3 showing the truncation rods of the ultrathin bonded sample. L (S) corresponds to the layer and substrate Bragg peak, A (B) corresponds to a tilt (twist) dislocation displacement peaks. Intensity scale is in counts/s.

of this function is based on two points: (i) the Fourier transform of a double-side exponential decay function $A_i \exp(-a_i|z|)$ in the real space is a Lorentzian function $2A_i a_i/(a_i{}^2+q_z^2)$ in the reciprocal space, (ii) the measured intensity is proportional to the square of the Fourier transform of the real space profile $I_i(q_z) \propto |F_i(q_z)|^2$. With this method, the strain field decrease rate along the normal is quantified with only one parameter, but the asymmetry due to the presence of the free surface[19] and the refraction effects due to the grazing emergence are not taken into account. Nevertheless, this treatment allows comparing the strain field decrease as the function of depth for each dislocation type. As shown in Fig. 5, this function is good enough to fit the data, so that it is difficult to justify a much complex function taking into account two different parameters for both sides of the exponential decay. For the TID (TWID) peaks noted A (B) in Fig. 4, we get $a_{\mathrm{TID}}=0.052$ Å^{-1} ($a_{\mathrm{TWID}}=0.056$ Å^{-1}) and $A_{\mathrm{TID}}=0.683$ ($A_{\mathrm{TWID}}=0.356$). It shows that the decrease rate of the dislocations strain fields near the (2,−2,0) reflection are nearly equivalent along the q_z direction for both dislocation types, but the effect at the surface is much stronger for TID than for TWID (see the inset of Fig. 5). This observation is explained by the dissociation of the TWID that gives an out-of-plane deformation. Indeed, a nondissociated pure screw dislocation should induce only an in-plane shear strain and no deformation along the surface normal.[19] In this sample, the dissociation length is about 33 Å compared to the film thickness of about 160 Å, so that the partials are well dissociated and quite close to the surface, and their summation gives an effective out-of-plane deformation. This assumption has been verified by isotropic continuum elasticity calculations. Moreover, TID's are not pure edge dislocations, giving the strongest effects on the surface deformation, but mixed dislocations having edge and screw component so that the deformation corresponding to (2,−2,0) reflection along the q_z direction is weakened. In this sample, the dislocation strain field is quite small on the surface (the surface values of the curves A and B drawn in the inset of Fig. 5 are, respectively, 2×10^{-4} and 5×10^{-5}). This is due to the strong screening of the strain fields of individual dislocation due to the large h/D ratio.[19] As confirmed by continuum elasticity calculation, decreasing the tilt and twist angles for the same thickness h of the film will decrease the screening and enhance the value of the strain field at the surface.

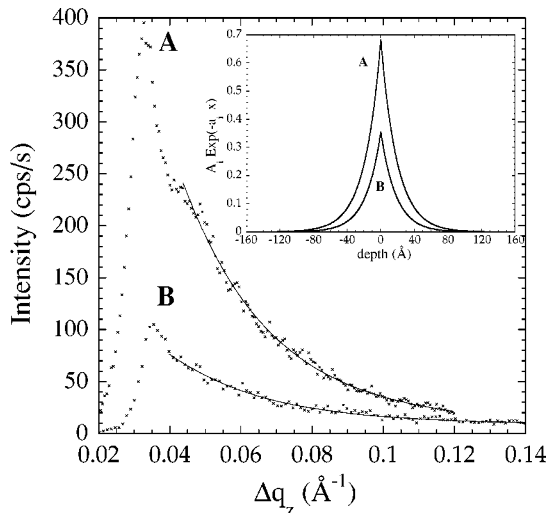

FIG. 5. Analysis of the intensity decrease of two truncation rods A and B corresponding to tilt and twist dislocation displacement peaks (see Fig. 4). The inset shows the result of the real-space strain field profile discussed in the text.

IV. CONCLUSIONS

Summarizing our work, we have presented in-plane and out-of-plane GIXRD measurements of the periodic strain field induced by "twist and tilt" dislocation networks obtained by ultrathin wafer bonding. The indexation of the sat-

ellite peaks due to the modulation of the in-plane atomic positions allows one to obtain very accurately the misalignment angles of the two wafers as well as the lateral periodicity of the supercell defined by the dislocation (square network for TWID's, average linear network for TID's). It has been pointed out that the instrumental resolution functionmust be taken into account and that several equivalent reflections must be measured. It has been shown that the strong interaction of dislocations (the periods are nearly equivalent) gives a very strong modulation of the peak intensities leading to the extinction of even (odd) satellite orders for TWID's (TID's). Moreover the efficiency to induce a deformation to the free surface has been estimated with the analysis of TR's. In this sample, the (layer thickness/dislocation lateral period) ratio is too large, and the dislocation strain field is strongly screened at the surface. All these results are useful to model the dislocation strain field to optimize the realization of new substrates allowing one to localize semiconductor quantum dots growth but also to obtain by selective chemical etching a nanometric patterning of the surfaces.[2,6,20] Some technological solutions are now proposed to control very accurately the twist and tilt angles.[21]

---

*Present address: HASYLAB, Notkestr. 85, D-22603 Hamburg, Germany.

[1] M. Bruel, Electron. Lett. **31**, 1201 (1995).

[2] F. Fournel, H. Moriceau, N. Magnea, J. Eymery, J. L. Rouviere, K. Rousseau, and B. Aspar, Mater. Sci. Eng., B **73**, 42 (2000).

[3] A. Bourret, Surf. Sci. **432**, 37 (1999).

[4] A. E. Romanov, P. M. Petroff, and J. S. Speck, Appl. Phys. Lett. **74**, 2280 (1999).

[5] F. Fournel, K. Rousseau, J. Eymery, J. L. Rouviere, D. Buttard, N. Magnea, H. Moriceau, B. Aspar, T. Baron, P. Mur, F. Martin, M. N. Sémeria (unpublished).

[6] M. Bruel, World patent No. 99/05711.

[7] J. G. Zhu and C. B. Carter, Philos. Mag. A **62**, 319 (1990); L. Sagalowicz, A. Rudra, A. Syrbu, J. Behrend, F. Salomonsson, K. Streubel, M. Hammar, and J. Bentell, Philos. Mag. Lett. **76**, 445 (1997).

[8] J. L. Rouvière, K. Rousseau, F. Fournel, and H. Moriceau, Appl. Phys. Lett. **77**, 1135 (2000).

[9] K. Rousseau, J. L. Rouviere, F. Fournel, and H. Moriceau, Mater. Sci. Semicond. Process. **4**, 101 (2001).

[10] J. Eymery, F. Fournel, H. Moriceau, F. Rieutord, D. Buttard, and B. Aspar, Appl. Phys. Lett. **75**, 3509 (1999).

[11] D. Buttard, J. Eymery, F. Fournel, K. Rousseau, R. Lazzari, and F. Leroy (unpublished).

[12] M. Nielsen, R. Feidenhans'l, P. B. Howes, J. Vedde, K. Rasmussen, M. Benamara, and F. Grey, Surf. Sci. **442**, L989 (1999).

[13] S. Weichel, F. Grey, K. Rasmussen, M. Nielsen, R. Feidenhans'l, P. B. Howes, and J. Vedde, Appl. Phys. Lett. **76**, 70 (2000).

[14] Q. Y. Tong and U. Gösele, *Semiconductor Wafer Bonding* (Wiley, New York, 1999).

[15] D. C. Champeney, *Fourier Transforms And Their Physical Applications* (Academic Press, London, 1973).

[16] R. Bonnet and J. L. Verger-Gaugry, Philos. Mag. A **66**, 849 (1992).

[17] D. M. Vardanyan and H. M. Petrosyan, Acta Crystallogr., Sect. A: Found. Crystallogr. **43**, 316 (1987).

[18] D^{TWID} is also calculated with Frank's relation $D^{\mathrm{TWID}} = |\mathbf{b}|/[2\sin(\psi/2)] = a_{\mathrm{Si}}/[2\sqrt{2}\sin(\psi/2)]$; F. C. Frank, *Defect in Crystalline Solids* (The Physical Society, London, 1954).

[19] J. Eymery, F. Fournel, K. Rousseau, D. Buttard, F. Leroy, F. Rieutord, and J. L. Rouviere, in *Dislocations and Deformation Mechanisms in Thin Films and Small Structures*, edited by O. Kraft *et al.*, MRS Symp. Proc. No. 673 (Materials Research Society, Warrendale, PA, 2001), p. 6.9.1.

[20] R. A. Wind, M. J. Murtagh, F. Mei, Y. Wang, M. A. Hines, and S. L. Sass, Appl. Phys. Lett. **78**, 2205 (2001).

[21] F. Fournel, H. Moriceau, B. Aspar, K. Rousseau, J. Eymery, J. L. Rouviere, and N. Magnea, Appl. Phys. Lett. **80**, 793 (2002).